
Article:
William, N, Nelson, L, Gutsell, S et al. (3 more authors) (2019) Hg-supported phospholipid monolayer as rapid screening device for low molecular weight narcotic compounds in water. Analytica Chimica Acta, 1069. pp. 98-107. ISSN 1873-4324

https://doi.org/10.1016/j.aca.2019.04.019

Accepted Manuscript

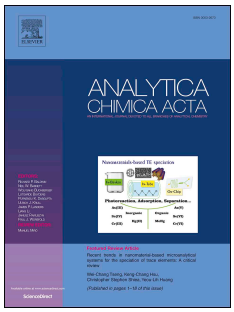

Hg-supported phospholipid monolayer as rapid screening device for low molecular weight narcotic compounds in water

N. William, A. Nelson, S. Gutsell, G. Hodges, J. Rabone, A. Teixeira

PII: S0003-2670(19)30428-3

DOI: https://doi.org/10.1016/j.aca.2019.04.019

Reference: ACA 236708

To appear in: *Analytica Chimica Acta*

Received Date: 14 February 2019

Revised Date: 4 April 2019

Accepted Date: 9 April 2019

Please cite this article as: N. William, A. Nelson, S. Gutsell, G. Hodges, J. Rabone, A. Teixeira, Hg-supported phospholipid monolayer as rapid screening device for low molecular weight narcotic compounds in water, *Analytica Chimica Acta*, https://doi.org/10.1016/j.aca.2019.04.019.

Hg-supported phospholipid monolayer as rapid screening device for low molecular weight narcotic compounds in water

N. William[a], A. Nelson[a]*, S. Gutsell[b], G. Hodges[b], J. Rabone[b], A. Teixeira[b]

[a]School of Chemistry, University of Leeds, Woodhouse lane, Leeds, LS2 9JT, UK.

[b]Safety and Environmental Assurance Centre, Unilever, Colworth Science Park, Sharnbrook, UK.

*corresponding author, e mail a.l.nelson@leeds.ac.uk, tel +441133436409

Abstract

This study positions the fabricated Pt/Hg-supported phospholipid sensor element in the context of more conventional biomembrane-based screening platforms. The technology has been used together with immobilised artificial membrane (IAM) chromatography and COSMOmic simulation methods to screen the interaction of a series of low molecular weight narcotic organic compounds in water with phosphatidylcholine (PC) membranes. For these chemicals it is shown that toxicity to aquatic species is related to compound hydrophobicity which is associated with compound accumulation in the phospholipid membrane as modelled by IAM chromatography measurements and COSMOmic simulations. In contrast, the Hg-supported dioleoyl phosphatidylcholine (DOPC) sensor element records membrane damage/modification which is indirectly related to general toxicity and directly related to compound structure. Electrochemical limit of detection (LoD) values depend on molecular structure and range from 20 μmol dm^{-3} for substituted phenols to 23 mmol dm^{-3} for aliphatics. Rapid cyclic voltammetry (RCV) "fingerprints" showed that the major structural classes of compounds: alkyl/chlorobenzenes, substituted phenols, quaternary ammonium compounds and neutral amines interacted distinctively with the DOPC on Hg and that these observations correlated with and supported those predicted by the COSMOmic simulations of the compound/DMPC association. In addition, the compatibility of the electrochemical and COSMOmic methods validates the electrochemical device as a meaningful high throughput technology to screen compounds in water and report on the mechanistic details of their interaction with phospholipid layers.

Keywords: Toxicity screening; Rapid cyclic voltammetry; Phospholipid layers; Immobilised artificial membranes; COSMOmic; Low molecular weight narcotics.

1. Introduction

Due to recent regulatory and cultural changes there is a growing need to replace *in vivo* toxicology testing of chemicals with *in vitro* and *in silico* models to better understand the mode of action and the biochemical pathways leading to an adverse outcome [1]. The toxic process of narcosis is believed to be a result of non-specific disturbance of the cell membrane (biomembrane) integrity and constitutes the minimal or "baseline" toxicity of every chemical [2]. Biomembranes also play a crucial role in the accumulation and distribution of chemicals in a biological system [3]. The logarithm of the octanol-water partition coefficient (log *P*) is often used as a parameter to estimate the partitioning of solutes into biomembranes [4,5], but for many chemicals (e.g. ionisable compounds and surfactants) octanol represents a poor surrogate for the anisotropic structure and complex molecular interactions occurring within the biological membrane [6]. In spite of this log *P* has a wide use in toxicology predictions and retains this significance as the log octanol-water partition coefficient throughout the text and tables of this paper. A number of biomembrane models and techniques are available that estimate more accurately the partitioning into biomembranes such as liposome-water partitioning [4], cell culture studies [7], nuclear magnetic resonance (NMR) [8], surface plasmon resonance spectroscopy [9], microscopic techniques [10], and theoretical molecular simulations [11,12]. However, these methods are often time- and cost-intensive and rarely suitable for routine high-throughput screening.

The Hg-supported dioleoyl phosphatidylcholine (DOPC) monolayer platform [13-16] using electrochemical interrogation has been employed as one successful biomembrane model. This model has recently been transferred to a high throughput platform and has been developed to screen organic compounds in water [13] but what it precisely measures in terms of compound-

biomembrane interaction is still uncertain. In contrast, two contemporary common techniques widely used for measuring compound-biomembrane interaction have been well characterised in terms of the parameters which they measure. These technologies are immobilised artificial membrane (IAM) chromatography and COSMOmic simulation. The stationary phase of the IAM column is comprised of porous silica particles coated with covalently linked dialkyl-phospholipids. The affinity of the compound of interest to the phospholipidic phase is determined from the retention factor which can be translated into a membrane-water partitioning value and has been shown to correlate well with values obtained through liposome-water partitioning [17,18]. COSMOmic [19] (a part of COSMOlogic software) is a fully predictive method that combines quantum chemistry and thermodynamics (COSMO-RS theory) [20] to calculate the free energy of molecules in their most favourable position and orientation in anisotropic systems. COSMOmic has been applied to predict the degree of partitioning of molecules in model membrane bilayers as well as their location in the lipid bilayer [19,21].

In the following, a systematic series of well-studied relatively low molecular weight aromatic and aliphatic compounds (Fig. 1) have been screened using these above three methods. This paper aims to validate the performance of the novel Hg-supported DOPC platform against the more established techniques of IAM [17] chromatography and COSMOmic simulation [19,21]. The aim is to define exactly which aspects of a compound-phospholipid interaction this technology measures. An additional objective is to see how the parameters derived from the supported layer platform relate to the mode of biological action of the narcotic compounds.

2. Materials and methods

2.1. Electrochemistry

2.1.1. Principle

Monolayers of DOPC on Hg undergo two potential-induced phase transitions characterised by two sharp capacitance current peaks respectively [13].These peaks correspond to the ingress of electrolyte into the layer and the re-organisation of the layer to form bilayer patches respectively [22-25]. Alterations of these capacitance peaks are synonymous to any changes in the monolayer structure [26]. Interaction of the selected compounds with the monolayer significantly influences the capacitance current-potential profile of the layer in a selective and systematic manner. A depression of the two peaks indicates an initial interaction of the compounds with the DOPC polar groups [27] whereas an increase in the capacitance current baseline reflects an association of a polar compound with the DOPC apolar region and/or its disruption [28]. On the other hand, penetration of compounds into the DOPC apolar region may affect the capacitance current baseline only slightly if they have a low polarisability, or they may even decrease the capacitance if they contribute to thickening or stiffening of the monolayer [29]. A potential shift of the capacitance peaks shows an alteration in potential profile across the layer implemented by the compound interaction [29,30]. A broadening of the peaks indicates an increase in monolayer disorder. Other workers have followed a similar but not *on-line* high throughput approach for example Becucci et al [31] indicated that changes of capacitance and resistance in the low capacitance potential domain of lipid on Hg drop electrodes represented phase transitions in the lipid mixtures. In addition the same workers [32] showed that the interaction of different monolayer-protected Au144 clusters at DOPC coated Hg gave rise to capacitance changes also in the low capacitance region of the voltammograms. Interestingly, the idea of using a lipid bilayer as an analytical sensor element has recently been developed in entirely separate systems [33].

All compounds studied in this paper contained no electroactive grouping since the resulting faradaic signal would interfere with the analysis described above.

2.1.2. Materials

Test compounds were obtained from Sigma-Aldrich. Their physical chemical properties [34-41] and generic toxicity to fish [42] expressed as −log LC_{50} are displayed in Table 1. LC_{50} represents the concentration of the chemical in water which kills 50% of the population of fathead minnow (*Pimephales promelas*) after 96 hours. Since low values of LC_{50} represent the most toxic compounds, the log LC_{50} value is expressed as a minus value for convenience of presentation so that the largest value of -log LC_{50} indicates the most toxic compound. Stock solutions were prepared in either acetone or 18.2 MΩ MilliQ water depending on solubility for final addition to test dilute working solutions in electrolyte. The electrolyte used throughout the experiments was 0.1 mol L^{-1} KCl, calcined at 600 ˚C for 2 h and buffered at pH 7.4 with 0.01 mol L^{-1} phosphate (hereinafter referred to as phosphate buffered saline or PBS). The DOPC was obtained from Avanti Polar Lipids Alabaster, AL, US and was >99% pure. The DOPC dispersion for electrode coating was prepared by gently shaking DOPC with PBS to give a 0.25 μmol mL^{-1} dispersion. All other reagents were of analytical grade and purchased from Sigma-Aldrich. The microfabricated platinum electrodes [43] (MPE) were supplied by the Tyndall National Institute, Ireland. Hg was electrodeposited on the Pt disc of radius 0.480 mm to give a Pt/Hg electrode as described previously [26,43].

2.1.3. Apparatus and procedure

For the assay, the reader is referred to ref [44] which gives a full description of the platform used and procedure which was carried out exactly as described previously. The approach has been used previously in more complex matrices of tap water and water with 3 mg dm^{-3} humic acid and has been shown to be free from interference [44]. In general the sensor gives distinctive responses to classes of compounds rather than individual compounds and mixtures of classes provide a generalised response which could be deconvolved in future studies. Specifically to this study, interactions of compounds with the DOPC monolayer were monitored by RCV while cycling the electrode potential from −0.4 to −1.2 V for 600 s during compound exposure. Following this, PBS

control electrolyte was introduced into the flow sensor module in place of the test compound in PBS. PBS was flushed through for 400 s with continued RCV cycling from −0.4 to −1.2 V to allow for any recovery of the DOPC layer's initial structure to occur. Both the screening and DOPC depuration are facilitated by an electrochemically induced rapid mobility of the DOPC across two reversible DOPC reorientations. In the cases of non-recovery an insignificant rate of removal of compound from the DOPC during the time scale of the experiment is indicated.

RCV plots were generated from the electrochemical experiments. Each RCV plot is a unique "fingerprint" characterising the interaction of each compound with the DOPC monolayer. In order to obtain a quantitative estimate of the effect of each compound on the DOPC layer, limits of detection (LoD) for the compound in PBS were estimated. The LoD is the minimum concentration of the compound in PBS which has a statistically significant effect on the monolayer's properties and is the quantitative analytical output from the RCV technology. Its experimental determination has been described in a previous paper [44]. The −log LoD values extracted for each compound/DOPC interaction in this study are displayed in Table 1. Due to the fact that the most active compounds on DOPC have the lowest LoD values, these were expressed as −log LoD. This was done for convenience of presentation so that the highest values of −log LoD represent the most active compound on the DOPC layer. Owing to the dynamic, induced mobility of the DOPC sensor element, the results from the RCV assay should relate to the way in which the compound/DOPC association influences the DOPC assembly.

2.2. IAM Chromatography

K_{IAM} for all compounds was determined by measuring the retention time on a Regis® Technologies IAM.PC.DD2 HPLC 100 mm x 4.6 id column. Measurements were performed using an Agilent LC 1200 series system equipped with refractive index detector (RID) and diode array detector (DAD). All compounds were analysed with isocratic elution by injecting 20 μL of a 0.5 to 1.7 mol L^{-1}

solution (or 0.14 to 0.34 mol L^{-1} for 1,2-dichlorobenzene, 1,2,4-trichlorobenzene and 2,4,6-tribromophenol) on to the column held at 25 °C and at a flow rate of 1 mL^{-1} min^{-1}. The aqueous eluent used consisted of 10 mmol L^{-1} ammonium acetate (pH 5.0) and PBS (pH 7.4) for 2,4,6-tribromophenol. Measurements were generally carried out at pH 5.0 to avoid interferences with the charged surface of the silica particles [45,46]. However, those done at pH 7.4 may suffer from interferences with the silica column surface. Due to the difference in pH between the IAM measurements (pH 5) and the electrochemical and toxicity studies (pH ~7.4), discrepancies in the ionisation states of the molecules, 2,4-dichlorophenol, 1,2-diaminoproprane and aniline may occur. For strongly sorbed compounds where no elution was obtained with 100% aqueous (aq) mobile phase, extrapolation was performed from at least three retention times of three different mobile phase ratios (aqueous/methanol). Log K_{IAM} 100% aq is equal to the intercept of the linear extrapolation curve. Log K_{IAM} is calculated based on the mean of the retention times of each standard (t_r) and an un-retained compound (t_0) using equation (1) below:

$$\log K_{IAM} = \log ((t_r - t_0)/t_0) \qquad (1)$$

The measured K_{IAM} values can be converted to a phospholipid-water partitioning coefficient ($K_{L/W}$) by accounting for the medium/phospholipid volume ratio of the column (0.053) [45]. $K_{L/W}$ is then simply calculated as:-

$$K_{L/W} = (K_{IAM} / 0.053) \qquad (2)$$

These values can be used as a direct descriptor of phospholipophilicity. Values for log $K_{L/W}$ obtained in this study are displayed in Table 1. Since the IAM reverse phase is composed of a phospholipid layer covalently attached to a silica bead, any interaction with a compound will involve a compound penetration step and will be directly related to the phospholipid affinity for the compound.

2.3. COSMOmic calculations

Principle and procedure.

Membrane partitioning calculations were performed using the COSMOmic [46-48] module of the COSMOtherm [49] software (version C30_1501). Time-averaged molecular dynamics (MD) trajectories using the CHARMM36 forcefield were used as the basis for the model of 1,2-dimyristoyl-sn-glycero-3-phosphocholine (DMPC) [47]. The output of this simulation was used to generate the DMPC micelle file, which was used in conjunction with TZVP-optimised structures of water and a representative DMPC phospholipid molecule to create a model of the DMPC membrane [50]. In this model, DMPC was simulated as a stack of 30 slabs of homogeneous fluids composed of the polar surfaces of the lipids and water molecules found within each slab. COSMOmic calculates the excess chemical potentials arising from the electrostatic, hydrogen bonding and dispersion interactions of the surface segments of the molecules within fluids. The chemical potentials of guest molecules in 162 orientations within the micelle model were then used to calculate free energies of interaction relative to water, from which distributions and membrane partition coefficients can be derived. For ionisable compounds, calculations were performed using both the neutral forms of the molecules and the ionised forms in combination with hydrated counter ions. For cations a hydrated bromide ion was used for the counter ion and for anions a hydrated sodium ion was used. This obviates the need to use a membrane potential in COSMOmic, with the advantage that the same ion pair can be used for partitioning calculations.

COSMOmic models micelles as stacks of homogeneous fluids, meaning that it will allow partitioning into individual slabs of the micelle in a manner that would in reality force the lipid molecules apart and require changes to their configuration. COSMOmic considers the volumes displaced by guest molecules within the slabs but has no mechanism to incorporate contributions from the stresses induced across slabs. A procedure was applied to adjust the free energies and distributions obtained from COSMOmic according to the differences between the guest molecule distributions and the lipid volume distributions [19]. The stress-corrected distributions differentiate between molecules that could fit within the micelle without causing reconfiguration of the lipid

molecules, and those which cannot. In addition to the calculated membrane partition coefficients, the distributions and free energies obtained from COSMOmic and the stress-corrected versions can be used to calculate mean free energies of interaction and residual misfit energies. These provide further information about the nature of the interaction between guest molecules and the membrane. COSMOmic helps to distinguish molecules which can interact strongly with lipid molecules but do not fit well into the membrane or interact with the polar head groups rather than the hydrocarbon chains. The simulation procedures can be used to obtain molecular profiles of concentrations of the DMPC molecule and the interacting molecule in a vertical section through the lipid layer. The compound profiles in the lipid layer are displayed with stress-correction. Another output from the COSMOmic simulations are mean lipid-water partition coefficients (log $K_{L/W}$ (*cosm*)) for each compound. Those displayed in Table 1 are calculated from the stress-corrected free energies with layers composed of greater than 95% water defined as outside the micelle. We are aware that the COSMOmic treatment is an approximation since it uses saturated DMPC not unsaturated DOPC as a model lipid although both phospholipids are fluid at 25^{o}. On the other hand, theoretical micelles are an implicit part of the COSMOmic membrane model in spite of the fact that DMPC micelles do not exist experimentally. However, all statements using the term "micelle" apply to membrane bilayers [18] and, since only the monolayer-compound interaction is of interest, the use of the theoretical micelle in the model is valid.

3. Results and discussion

3.1. Electrochemical, IAM, log *P* and toxicological correlations.

Fig. 2 shows the relationships between, (a) log $K_{L/W}$ and log *P* [41] and between (b) log $K_{L/W}$ and log $K_{L/W}$(*cosm*). In addition, correlations are displayed between -log LC_{50} values from reference [42] and (c) –log LoD and, (d) log $K_{L/W}$ values and between (e) –log LoD and log $K_{L/W}$. In all cases the best linear fit is drawn through the data with the multiple R 95% correlation coefficient value shown. The log $K_{L/W}$ set of data has a close relationship with log *P* (Fig. 2(a)) which indicates that

log $K_{L/W}$ is directly related to the organic partitioning of the compounds. However, the correlation between log $K_{L/W}$ and log P has not always been experimentally observed [46]. The tight correlation between log $K_{L/W}$ and log $K_{L/W}$(*cosm*) (Fig. 2(b)) validates the use of the COSMOmic simulations as a method to predict compound-lipid partitioning. Significantly, in this case the slope of the best fit line is close to unity (1.00) with an intercept close to zero (-0.01). The correlation between –log LC_{50} and –log LoD (Fig. 2(c)) is positive but not tight (R=0.65). Significantly there is a closer linear relationship (R=0.92) between –log LC_{50} and log $K_{L/W}$ (Fig. 2(d)) indicating that the toxicity of the compounds is related to their affinity for the organic phase. This relationship and the empirical reasons for it have been well established [51] and indicate that a non-specific and narcotic toxic mode of action is linked to the generic partitioning and accumulation of compounds into biological membranes [52-54]. The reason for the weaker relation between –log LC_{50} and –log LoD is that the LoD measurement represents the lowest aqueous concentration of compound which structurally modifies the DOPC layer. This is indirectly related to biomembrane partitioning as confirmed by the weaker relationship between –log LoD and log $K_{L/W}$ (Fig. 2(e)). Biomembrane modification is therefore not necessarily directly associated with non-specific toxicity and narcosis.

The differing outputs of the IAM and the RCV experiments are expected in view of the way the experiments are carried out. IAM employs a monolayer of phospholipid covalently attached to a silica bead. In contrast the monolayer of DOPC on Hg is highly mobile and its mobility and full exposure to the aqueous phase is maintained during :- (a) the electrochemical scanning throughout the assay and, (b) the DOPC depuration procedure. As a result, the IAM assay contains a penetration element in the affinity of the compound for the phospholipid layer. On the other hand, the RCV measurement gives information on the way and the extent to which the compound self-assembles in the DOPC layer and how this affects the structure of the mobile DOPC phase.

3.2. RCV plots and COSMOmic simulations

The effects of the interactions of the compounds with the DOPC monolayer on the capacitance current-potential (RCV) plots are presented in this section together with the COSMOmic simulation of the interaction of the same compounds with DMPC micelles. From these observed effects specific patterns led us to subdivide the compounds into separate classes and discuss them as such. The classes are, (i) alkyl/chlorobenzenes, (ii) substituted phenols, (iii) cationic aromatic and (iv) neutral amines.

Fig. 3 shows the RCV plots and COSMOmic simulations resulting from the compound/lipid interactions representative of the alkyl/chlorobenzenes and substituted phenol compounds. The RCV plots show a clear difference between the interaction of the two compound groups with the DOPC monolayer. The alkyl/chlorobenzene interaction with DOPC initiates a significant shift of capacitance current peaks 1 and 2 to more negative potentials accompanied by a peak depression. On the other hand, the substituted phenol/DOPC interaction gives rise to a depression of both capacitance peaks with minimal potential shift. 2,4-dichlorophenol interaction causes a peak broadening indicating an increase of disorder in the DOPC layer. The negative potential shift in the RCV following alkyl/chlorobenzene interaction with DOPC is common to all aromatic/DOPC interactions and is indicative of these compound's association with a phospholipid monolayer [44]. This effect is dependent on the concentration of the compound [44] and the extent of compound substitution as in ethylbenzene and 1,2,4-trichlorobenzene.

It is significant that following interaction with the more highly substituted alkyl/chlorobenzene compounds in the electrochemical model, the DOPC layer structure and organisation cannot be recovered after flushing with PBS whilst scanning from −0.4 to −1.2 V (Fig. 3 and Table 1)). This shows that these compounds are irreversibly bound to the DOPC layer within the operational range of the experiment. This effect may be related to the decreased water solubility of the higher

substituted compounds (see Table 1). A decreased water solubility will impede the transfer of the compound from the DOPC association to the surrounding electrolyte and could be the main factor leading to an increased log *P* of these compounds. In contrast, there is complete recovery of the DOPC layer following *o*-cresol/DOPC and 2,4,6-tribromophenol/DOPC interactions and subsequent flushing with PBS (Fig. 3 and Table 1). Note the change in the RCV plot following interaction when the -Cl group in 1,2,4-trichlorobenzene is replaced by -OH in 2,4-dichlorophenol (Fig. 3). In this case, unlike the 1,2,4-trichlorobenzene/DOPC interaction, there is partial recovery of the DOPC layer after PBS flushing. The recovery of the DOPC layer following 2,4,6-tribromophenol interaction is surprising in view of the low water solubility and the high log *P* of 2,4,6-tribromophenol (Table 1). Consequently, the relatively rapid rate of depuration must relate to another property of the molecule in comparison with the more highly substituted alkyl/chlorobenzenes. One possibility is that the presence of the -OH group enables a more rapid transfer of 2,4,6-tribromophenol to the aqueous phase.

The results from the COSMOmic simulation are also displayed in Fig. 3 and indicate that the alkyl/chlorobenzenes fit well into the DMPC monolayer and are distributed evenly between the polar groups and apolar chains extending the full length of the lipid molecule. Owing to the static nature of the model, the COSMOmic simulations are not sensitive enough to distinguish the degrees of interaction for each substituted compound. The results of the COSMOmic simulation generally indicate that the phenols have a more restricted location in the DMPC micelle and do not extend the full length of the alkyl chains. This accounts for the increased disruption of the DOPC layer observed in the RCV representing the 2,4-dichlorophenol/DOPC interaction. The 2,4,6-tribromophenol/DMPC interaction is significant since its simulated molecular profile in the DMPC layer approaches that arising from the alkyl/chlorobenzene interaction in its ability to extend the whole thickness of the lipid layer. This is commensurate with the decreased disruption to the RCV plot following tribromophenol/DOPC interaction.

Fig. 4 displays RCV plots and COSMOmic simulations resulting from benzyltrimethylammonium ion, benzylamine and 1,2-diaminopropane interaction with DOPC on Hg and DMPC micelles respectively. Benzyltrimethylammonium ion interaction with the DOPC layer effects a shift of the capacitance current peaks to positive potential (Fig. 4(a)). This can be related to the positively charged compound adsorbing on the DOPC layer surface and has been observed previously as a response to the adsorption of positively charged inorganic ions [55]. Benzylamine interacts at lower solution concentrations in the same way as the benzyltrimethylammonium ion causing a positive potential shift in the two capacitance current peaks (see Fig. 4(b)). Benzylamine with a pK_a of 9.34 (see Table 1) is ~99% protonated at pH 7.4 and adsorption of benzylammonium ions within the polar head region is predicted [55]. The location of the benzyltrimethylammonium and benzylammonium ions within the DMPC polar head region is quite clear from the COSMOmic simulations (Figs. 4(a) and (b)) as a restricted location within the outer half of the DMPC layer [47]. It is significant that following interaction with the benzyltrimethylammonium chloride and the benzylammonium ions, the DOPC layer structure and organisation can be recovered after flushing with PBS whilst voltage scanning from −0.4 to −1.2V indicating that the compound interaction is reversible entailing no loss of DOPC from the electrode surface.

The interaction of benzylamine with the DOPC on Hg is altered at higher solution concentrations of benzylamine with a complete suppression of the capacitance peaks and a large increase in the baseline capacitance current at less negative potentials (Fig.4(c)). A similar interaction with DOPC is observed from 1,2-diaminopropane of pK_a 9.84 (Fig. 4(d)). The structureless features of the baseline capacitance current increase in both cases can be ascribed to a disruption of the DOPC film. The increased concentration of the ~1% neutral benzylamine and <1% 1,2-diaminopropane are the active moieties [56,57] which penetrate and disrupt the DOPC layer. The COSMOmic profile of neutral benzylamine and 1,2-diaminopropane in the DMPC micelle is commensurate

with this showing a deeper penetration of the DMPC layer with an uneven profile leading to layer disruption.

Following benzylamine and 1,2-diaminopropane interaction with DOPC and flushing of the DOPC layer whilst voltage scanning from −0.4 to −1.2 V, no recovery of the DOPC layer is observed showing that the interaction is operationally irreversible. Both benzylamine and 1,2-diaminopropane possess a relatively low log *P* and finite water solubility (Table 1) which is counter-intuitive to the observed irreversibility. However, a strong interaction between the amine grouping and the lipid polar groups through H-bonding together with a layer disruption could impede the transfer to the aqueous phase. These compounds are classed as amine narcotics which have a toxicity above that of baseline narcotics [58-60] a fact which might explain their irreversible interaction with the biomembrane model. By the same token, ethanolamine (pK_a 9.5) interacts with DOPC and the interaction is partly reversible (Table 1). Significantly, however, aniline's interaction with the DOPC layer is reversible (Table 1). Aniline is not classed as an amine narcotic and its H-bonding ability is compromised through delocalisation of the lone pair of electrons on the N atom with the benzene ring.

4. Conclusions

1.This study positions the electrochemical biomembrane model (RCV) within the landscape of conventional compound and pharmaceutical screeners in water. In particular the model is shown to provide insights into membrane modification and compound class specific interaction: two processes which are not captured by chromatographic partitioning measurement technologies such as HPLC-IAM. Also evident is that, whereas IAM partitioning data correlates closely with fish narcosis for a set of low molecular weight organic compounds, the RCV LoDs correlate less well with narcosis for the same set of compounds. This indicates that membrane modification is only indirectly related to narcosis. Indeed while membrane partitioning is an exact thermodynamic

quantity, LoD values contain a factor relating to the membrane modifying capacity in addition to a membrane-partitioning factor.

2. The results from this study using RCV together with COSMOmic simulation show the following. Alkyl/chlorobenzenes form associations with the PC layer with little disruption of, and good fit in, the layer structure. The irreversibility of the interaction of the molecule with the layer is related to the degree of aromatic substitution. Substituted phenols interact reversibly with PC layers introducing layer disruption associated with a more restricted distribution and less good molecular fit than the alkyl/chlorobenzenes. The benzyltrimethylammonium and benzylammonium ions adsorb within the polar head groups of PC layers. At higher solution concentrations the neutral benzylamine and 1,2-diaminopropane is associated irreversibly with the DOPC layers in addition to introducing a layer disruption.

5. Acknowledgements

We would like to thank Elin Barrett for the further advice and comments given in the COSMOmic section and Mike Pleasants for initiating the collaboration between the two groups. Thanks to Edward Yorke for preparing the final COSMOmic plots. This work was supported by NERC (UK) grant NE/M021378/1 and latterly by the EU HORIZON 2020 HISENTS programme grant agreement number 685817.

6. References

[1] Committee on Toxicity Testing and Assessment of Environmental Agents, and National, R. C., Toxicity Testing in the 21st Century: A Vision and a Strategy, The National Academies Press, 2007.

[2] K.U.Goss, K. Bittermann, L. Henneberger, L. Linden, Equilibrium biopartitioning of organic anions – A case study for humans and fish, Chemosphere 199 (2018) 174-181.

[3] S. Fujisawa, T. Atsumi, Y. Kadoma, Cytotoxicity of methyl methacrylate (MMA) and related compounds and their interaction with dipalmitoylphosphatidylcholine (DPPC) liposomes as a model for biomembranes, Oral Diseases 6 (2000) 215-221.

[4] B.I.Escher, R.P.Schwarzenbach, Partitioning of substituted phenols in liposome-water, biomembrane-water, octanol-water systems, Environmental Science & Technology, 30 (1995)260-270.

[5] E.Urrestarazu Ramos, W.H.Vaes, H.J.Verhaar, J.L.Hermens, Quantitative structure- activity relationships for the aquatic toxicity of polar and nonpolar narcotic pollutants. Journal of chemical information and computer sciences 38 (1998) 845-52.

[6] A.D.Gunatilleka, C.F.Poole, Models for estimating the non-specific toxicity of organic compounds in short-term bioassays, Analyst 125 (2000)127-32.

[7] H.Glatt,I.Gemperlein, G.Turchi, H.Heinritz, J.Doehmer, F.Oesch,Search for cell culture systems with diverse xenobiotic-metabolizing activities and their use in toxicological studies, Molecular Toxicology 1 (1987) 313-34.

[8] M.Herve, J.C.Debouzy, E.Borowski, B.Cybulska, C.M.Gary-Bobo,The role of the carboxyl and amino groups of polyene macrolides in their interactions with sterols and their selective toxicity. A 31P-NMR study, Biochimica et Biophysica Acta (BBA)-Biomembranes 980 (1989) 261-72.

[9] A.Dahlin, M.Zäch, T.Rindzevicius, M.Käll, D.S.Sutherland, F.Höök,Localized surface plasmon resonance sensing of lipid-membrane-mediated biorecognition events, Journal of the American Chemical Society 127 (2005) 5043-8.

[10] N.Gal, D.Malferarri, S.Kolusheva, P.Galletti, E.Tagliavini, R.Jelinek,Membrane interactions of ionic liquids: Possible determinants for biological activity and toxicity, Biochimica et Biophysica Acta (BBA)-Biomembranes 1818 (2012) 2967-74.

[11] M.N.Jones ,Surfactant interactions with biomembranes and proteins. Chemical Society Reviews 21 (1992) 127-36.

[12] T.W.Sirk, E.F.Brown, M.FrieLan, A.K.Sum. Molecular binding of catechins to biomembranes: relationship to biological activity, Journal of Agricultural and Food Chemistry 57 (2009) 6720-8.

[13] A.Nelson A. Electrochemistry of mercury supported phospholipid monolayers and bilayers, Current Opinion in Colloid and Interface Science 15(2010) 455-66.

[14] A.Nelson, N.Auffret, Phospholipid monolayers of di-oleoyl lecithin at the mercury/water interface, Journal of Electroanalytical Chemistry and Interfacial Electrochemistry 244 (1988) 99-113.

[15] A.Nelson, A.Benton, Phospholipid monolayers at the mercury/water interface, Journal of Electroanalytical Chemistry and Interfacial Electrochemistry 202 (1986) 253-70.

[16] D.Bizzotto, A.Nelson,Continuing electrochemical studies of phospholipid monolayers of dioleoyl phosphatidylcholine at the mercury- electrolyte interface, Langmuir 14(1998) 6269-73.

[17] C.Pidgeon, S.Ong, H.Liu, X.Qiu, M.Pidgeon, A.H.Dantzig, J.Munroe, W.J.Hornback, J.S.Kasher, IAM chromatography: an *in vitro* screen for predicting drug membrane permeability, Journal of Medicinal Chemistry 38 (1995) 590-4.

[18] A.Taillardat-Bertschinger, C.A.Martinet, P.A.Carrupt, M.Reist, G.Caron, R.Fruttero, B.Testa, Molecular factors influencing retention on immobilized artificial membranes (IAM) compared to partitioning in liposomes and n-octanol, Pharmaceutical Research 19 (2002) 729-37.

[19] A.Klamt, U.Huniar, S.Spycher, J.Keldenich, COSMOmic: a mechanistic approach to the calculation of membrane-water partition coefficients and internal distributions within membranes and micelles, The Journal of Physical Chemistry B, 112 (2008)12148-57.

[20] A.Klamt, Conductor-like screening model for real solvents: a new approach to the quantitative calculation of solvation phenomena, The Journal of Physical Chemistry 9 (1995) 2224-2235.

[21] K.Bittermann, S.Spycher, S.Endo, L.Pohler, U.Huniar, K.U.Goss, A.Klamt, Prediction of phospholipid–water partition coefficients of ionic organic chemicals using the mechanistic model COSMOmic, The Journal of Physical Chemistry B 118 (2014) 14833-42.

[22] F.A.M.Leermakers, A.Nelson, Substrate-induced structural changes in electrode-adsorbed lipid layers: a self-consistent field theory, Journal of Electroanalytical Chemistry and Interfacial Electrochemistry 278 (1990) 53-72.

[23] A.Nelson, F.A.M.Leermakers, Substrate-induced structural changes in electrode-adsorbed lipid layers: experimental evidence from the behaviour of phospholipid layers on the mercury-water interface, Journal of Electroanalytical Chemistry and Interfacial Electrochemistry 278 (1990) 73-83.

[24] Brukhno AV, Akinshina A, Coldrick Z, Nelson A, Auer S. Phase phenomena in supported lipid films under varying electric potential, Soft Matter 7 (2011)1006-17.

[25] Vakurov A, Galluzzi M, Podesta A, Gamper N, Nelson AL, Connell SD. Direct characterization of fluid lipid assemblies on mercury in electric fields. ACS nano 8 (2014) 3242-50.

[26] Coldrick Z, Steenson P, Millner P, Davies M, Nelson A. Phospholipid monolayer coated microfabricated electrodes to model the interaction of molecules with biomembranes, Electrochimica Acta 54 (2009) 4954-62.

[27] Vakurov A, Brydson R, Nelson A. Electrochemical modeling of the silica nanoparticle–biomembrane interaction, Langmuir 28 (2011) 1246-55.

[28] N.Ormategui, S.Zhang, I.Loinaz, R.Brydson, A.Nelson, A.Vakurov, Interaction of poly (N-isopropylacrylamide)(pNIPAM) based nanoparticles and their linear polymer precursor with phospholipid membrane models, Bioelectrochemistry 87 (2012) 211-9.

[29] A.Nelson, N.Auffret and J.Borlakoglu, Interaction of hydrophobic organic compounds with mercury adsorbed dioleoyl phosphatidylcholine monolayers, Biochim. Biophys. Acta 1021 (1990) 205-216.

[30] A.Rashid, A.Vakurov, S.Mohamadi, D.Sanver, A.Nelson, Substituents modulate biphenyl penetration into lipid membranes, Biochimica et Biophysica Acta (BBA)-Biomembranes 1859 (2017) 712-21.

[31] L.Becucci, S. Martinuzzi, E. Monetti, R. Mercatelli, F. Quercioli, D. Battistel, R.Guidelli, Electrochemical impedance spectroscopy and fluorescence lifetime imaging of lipid mixtures self-assembled on mercury, Soft Matter 6 (2010) 2733-2741.

[32] L.Becucci, R.Guidelli, F.Polo, F. Maran, Interaction of mixed-ligand monolayer-protected au144 clusters with biomimetic membranes as a function of the transmembrane potential, Langmuir 30 (2014) 8141-8151.

[33] X. Wang, S. Ma, Y. Su, Y. Zhang, H. Bi, L. Zhang and X. Han, High impedance droplet–solid interface lipid bilayer membranes, Analytical Chemistry 87 (2015) 2094-2099.

[34] A.Seidell,Solubilities of Organic Compounds. Vol. II, D. Van Nostrand Company, Inc., New York, 1941.

[35] S.H.Yalkowsky, Y.He, P.Jain,Handbook of Aqueous Solubility Data, 2nd Edit, 2010.

[36] A.L.Horvath, F.W.Getzen, Z.Maczynska, IUPAC-NIST solubility data series 67. Halogenated ethanes and ethenes with water, Journal of Physical and Chemical Reference Data, 28 (1999) 395-627.

[37] G.R.Southworth, J.L.Keller, Hydrophobic sorption of polar organics by low organic carbon soils, Water, Air, and Soil Pollution 28 (1986) 239-48.

[38] D.R.Lide, Handbook of Chemistry and Physics, 88th ed. CRC Press, Boca Raton, FL, 2007.

[39] E.P.Serjeant, B. Dempsey, Ionisation Constants of Organic Acids in Aqueous Solution. International Union of Pure and Applied Chemistry (IUPAC). IUPAC Chemical Data Series No. 23, 1979.

[40] D.D.Perrin, Ionisation Constants of Inorganic Acids and Bases in Aqueous Solution, Elsevier, 2016.

[41] C.Hansch, A.Leo, D.Hoekman, D.J.Livingstone, Exploring QSAR: Hydrophobic, Electronic, and Steric Constants, Washington, DC, American Chemical Society,1995.

[42] C.L.Russom, S.P.Bradbury, S.J.Broderius, D.E.Hammermeister, R.A.Drummond, Predicting modes of toxic action from chemical structure: acute toxicity in the fathead minnow (Pimephales promelas), Environmental Toxicology and Chemistry16 (1997) 948-67.

[43] Z.Coldrick, A.Penezić, B.Gašparović, P.Steenson, J.Merrifield, A.Nelson, High throughput systems for screening biomembrane interactions on fabricated mercury film electrodes, Journal of Applied Electrochemistry 41(2011) 939-49.

[44] S.Mohamadi, D.J.Tate, A.Vakurov, A.Nelson, Electrochemical screening of biomembrane-active compounds in water, Analytica Chimica Acta 813 (2014) 83-9.

[45] F.Barbato, The use of immobilised artificial membrane (IAM) chromatography for determination of lipophilicity, Current Computer-Aided Drug Design 2 (2006) 341-52.

[46] S.T.Droge, J.L.Hermens, J.Rabone, S.Gutsell, G.Hodges, Phospholipophilicity of $C_x H_y N^+$ amines: chromatographic descriptors and molecular simulations for understanding partitioning into membranes, Environmental Science: Processes and Impacts 18 (2016) 1011-23.

[47] S.Jakobtorweihen, T.Ingram, I.Smirnova, Combination of COSMOmic and molecular dynamics simulations for the calculation of membrane–water partition coefficients, Journal of Computational Chemistry 34 (2013)1332-40.

[48] R.B.Best, X.Zhu, J.Shim, P.E.M.Lopes, J.Mittal, M.Feig, A.D. MacKerell Jr., Optimization of the additive CHARMM all-atom protein force field targeting improved sampling of the backbone ϕ, ψ and side-chain $\chi1$ and $\chi2$ dihedral angles, Journal of Chemical Theory and Computation 8 (2012) 3257-3273.

[49] F.Eckertand A.Klamt, Version C3. 0, Release 13.01. COSMOlogic GmbH & Co, KG, 2010.

[50] S.T.Droge, J.L.Hermens, S.Gutsell, J.Rabone, G.Hodges,. Predicting the phospholipophilicity of monoprotic positively charged amines, Environmental Science: Processes and Impacts 19 (2017) 307-23.

[51] W.H.J.Vaes, E.U.Ramos, H.J.M.Verhaar, J.L.M.Hermens, Acute toxicity of nonpolar versus polar narcosis: Is there a difference? Environmental Toxicology and Chemistry 17 (1998) 1380-1384.

[52] N.Timmer, S.T.Droge, Sorption of cationic surfactants to artificial cell membranes: comparing phospholipid bilayers with monolayer coatings and molecular simulations, Environmental Science and Technology 51(2017) 2890-8.

[53] H.Könemann, Quantitative structure-activity relationships in fish toxicity studies Part 1: Relationship for 50 industrial pollutants, Toxicology 19 (1981) 209-21.

[54] J.Sikkema, J.A.de Bont, B.Poolman, Interactions of cyclic hydrocarbons with biological membranes, Journal of Biological Chemistry 269 (1994) 8022-8.

[55] A.Rashid, A.Vakurov, A.Nelson, Role of electrolyte in the occurrence of the voltage induced phase transitions in a dioleoyl phosphatidylcholine monolayer on Hg, Electrochimica Acta 155 (2015) 458-65.

[56] J.K.Seydel, V.M.Albores, E.A.Coats, H.P.Cordes, B.Kunz, M.Wiese, The importance of drug-membrane interaction in drug research and development, Molecular Informatics 11 (1992) 205-10.

[57] H.N.Christensen, M.Liang, Modes of uptake of benzylamine by the Ehrlich cell, Journal of Biological Chemistry 241 (1966) 5552-6.

[58] G.D.Sinks, T.A.Carver, T.W.Schultz, Structure-toxicity relationships for aminoalkanols: a comparison with alkanols and alkanamines, SAR and QSAR in Environmental Research 9 (1998) 217-28.

[59] S.Ren, P.D.Frymier, T.W.Schultz, An exploratory study of the use of multivariate techniques to determine mechanisms of toxic action, Ecotoxicology and Environmental Safety 55 (2003) 86-97.

[60] T.W.Schultz, J.S.Jaworska, R.S.Hunter, Volume fraction analyses for selected mechanisms of toxic action, In Environmental Toxicology and Risk Assessment: Third Volume, ASTM International, 1995.

Figure Captions

Fig. 1

Compounds and their structures investigated; (a) 2,4-dichlorophenol, (b) *o*-cresol, (c) benzamide, (d) benzylamine, (e) benzyltrimethylammonium ion, (f) toluene, (g) diethyleneglycol, (h) 2-butanone, (i) trichloroethene, (j) 1,2-dichlorobenzene, (k) 1,2,4-trichlorobenzene, (l) ethylbenzene, (m) 2,4,6-tribromophenol, (n) 1,2-diaminopropane, (o) aniline, (p) ethanolamine.

Fig. 2

Plots of; (a) log $K_{L/W}$ vs log P, and (b) log $K_{L/W}$ vs log $K_{L/W}$ (*cosm*) for all compounds, (c) –log (LC_{50} / mol L^{-1}) vs –log (LoD/mmol L^{-1}), (d) –log (LC_{50}/mol L^{-1}) vs log $K_{L/W}$ and (e) –log (LoD/mmol L^{-1}) vs log $K_{L/W}$. The 95% multiple correlation coefficient R value is displayed on each plot.

Fig. 3

RCV recorded of a DOPC coated Pt/Hg (black line) in the presence of 5 mmol L^{-1} ethylbenzene, 1 mmol L^{-1} 1,2,4-trichlorobenzene, 1 mmol L^{-1} 2,4-dichlorophenol and 1 mmol L^{-1} 2,4,6-tribromophenol (red line), and recovery (blue line) in 0.1 mol L^{-1} PBS at pH 7.4. Right panel shows COSMOmic data for distribution of DMPC molecule (black line) and compounds with misfit correction (blue line) in DMPC micelle.

Fig. 4

RCV recorded of a DOPC coated Pt/Hg (black line) in the presence of, (a) 5 mmol L^{-1} benzyltrimethylammonium chloride and, (b) 0.5 and (c) 10 mmol L^{-1} benzylamine and (d) 25 diaminopropane (red line) and, recovery (blue line) in 0.1 mol L^{-1} PBS at pH 7.4. Right panel

shows COSMOmic data for distribution of DMPC molecule (black line) and compounds with misfit correction (blue line) in DMPC micelle.

Table 1. Compounds investigated: physical and chemical properties and parameters measured

Compound	log (water solubility/ mg L^{-1}) [34-37]	DM/ Debye [38]	pK_a [39,40]	log $K_{L/W}$ (*cosm*)	log *P* (exp't'l) [41]	−log (LC_{50}/mol L^{-1}) [42]	log $K_{L/W}$ (IAM)	−log (LoD/mmol L^{-1})	Reversibility interaction with DOPC
Toluene	2.72	0.375		2.9	2.73	3.43	2.46	−0.176	Rev
Ethylbenzene	2.23	0.59		3.17	3.15	4.00	3.59	−0.44716	Irrev
1,2-Dichlorobenzene	1.90	2.5		3.31	3.43	4.19	4.06	−0.204	Irrev
1,2,4-Trichlorobenzene	1.69			3.4	4.02	4.78	4.52	0.69897	Irrev
o-Cresol	4.41	1.45		3.28	1.95	3.89	2.67	0	Rev
2,4-Dichlorophenol	3.65		7.89	4.34	3.06	4.32	3.93	1.69	Partly rev
2,4,6-Tribromophenol	1.84		6.8	4.97	4.13	4.70	4.927	1	Rev
Benzyltrimethylammonium Cl	5.28			0.7			0.775	0.522	Rev
Benzylamine	6		9.34	1.18	1.09	3.02	0.89	0.602	Rev/irrev
Aniline	4.56	1.13	4.6	2.01	0.9	2.99	1.45	−1.06	Rev
Benzamide	4.13	12.2		1.11	0.64	2.26	1.54	−0.301	Rev
2-Hydroxyethylether	6	2.31		−0.42	−1.47	0.15	−0.312	−1.08	Rev
2-Butanone	5.35	2.779		0.66	0.29	1.35	0.862	0	Rev
1,2-Diaminopropane	6		9.82	−0.1	−1.2	1.87	−0.318	−0.301	Irrev
2-Aminoethanol	6	2.27	9.50	0.25	−1.31	1.47		−1.36	Partly rev
Trichloroethylene	3.11			2.92	2.61	3.47	2.33	−0.602	Rev

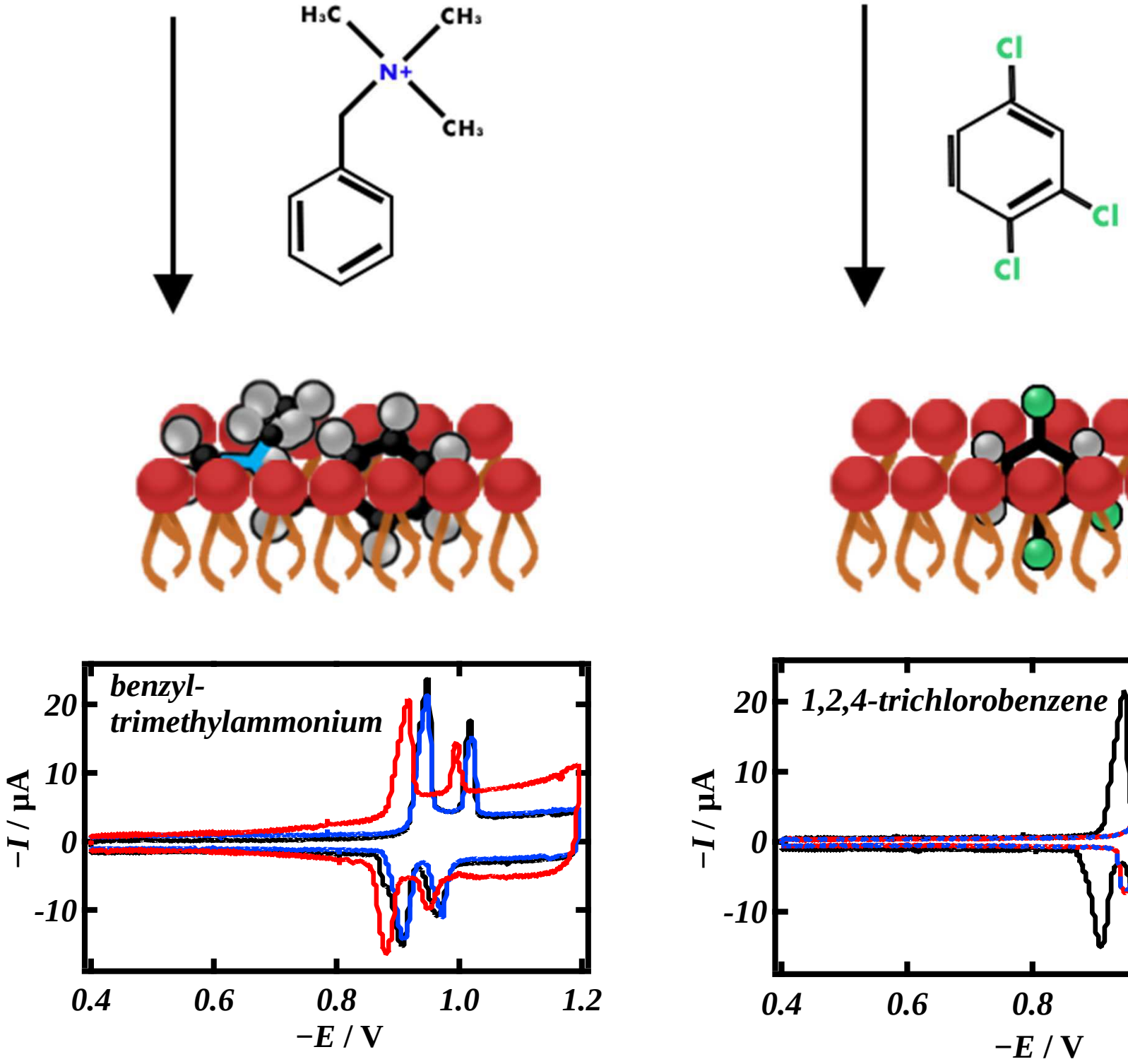
H₃C
CH₃
N+
CH₃
Cl
Cl
Cl
benzyl-
trimethylammonium
1,2,4-trichlorobenzene
20
10
0
-10
−I / µA
0.4
0.6
0.8
1.0
1.2
−E / V

Table 1. Compounds investigated: physical and chemical properties and parameters measured

Compound	log (water solubility/ mg L^{-1}) [34-37]	DM/ Debye [38]	pK_a [39,40]	log $K_{L/W}$ (*cosm*)	log *P* (exp't'l) [41]	–log (LC_{50}/mol L^{-1}) [42]	log $K_{L/W}$ (IAM)	–log (LoD/mmol L^{-1})	Reversibility interaction with DOPC
Toluene	2.72	0.375		2.9	2.73	3.43	2.46	–0.176	Rev
Ethylbenzene	2.23	0.59		3.17	3.15	4.00	3.59	–0.44716	Irrev
1,2-Dichlorobenzene	1.90	2.5		3.31	3.43	4.19	4.06	–0.204	Irrev
1,2,4-Trichlorobenzene	1.69			3.4	4.02	4.78	4.52	0.69897	Irrev
o-Cresol	4.41	1.45		3.28	1.95	3.89	2.67	0	Rev
2,4-Dichlorophenol	3.65		7.89	4.34	3.06	4.32	3.93	1.69	Partly rev
2,4,6-Tribromophenol	1.84		6.8	4.97	4.13	4.70	4.927	1	Rev
Benzyltrimethylammonium Cl	5.28			0.7			0.775	0.522	Rev
Benzylamine	6		9.34	1.18	1.09	3.02	0.89	0.602	Rev/irrev
Aniline	4.56	1.13	4.6	2.01	0.9	2.99	1.45	–1.06	Rev
Benzamide	4.13	12.2		1.11	0.64	2.26	1.54	–0.301	Rev
2-Hydroxyethylether	6	2.31		–0.42	–1.47	0.15	–0.312	–1.08	Rev
2-Butanone	5.35	2.779		0.66	0.29	1.35	0.862	0	Rev
1,2-Diaminopropane	6		9.82	–0.1	–1.2	1.87	–0.318	–0.301	Irrev
2-Aminoethanol	6	2.27	9.50	0.25	–1.31	1.47		–1.36	Partly rev
Trichloroethylene	3.11			2.92	2.61	3.47	2.33	–0.602	Rev

Table 1. Compounds investigated: physical and chemical properties and parameters measured

Compound	log (water solubility/ mg L^{-1}) [34-37]	DM/ Debye [38]	pK_a [39,40]	log $K_{L/W}$ (*cosm*)	log *P* (exp't'l) [41]	–log (LC_{50}/mol L^{-1}) [42]	log $K_{L/W}$ (IAM)	–log (LoD/mmol L^{-1})	Reversibility interaction with DOPC
Toluene	2.72	0.375		2.9	2.73	3.43	2.46	–0.176	Rev
Ethylbenzene	2.23	0.59		3.17	3.15	4.00	3.59	–0.44716	Irrev
1,2-Dichlorobenzene	1.90	2.5		3.31	3.43	4.19	4.06	–0.204	Irrev
1,2,4-Trichlorobenzene	1.69			3.4	4.02	4.78	4.52	0.69897	Irrev
o-Cresol	4.41	1.45		3.28	1.95	3.89	2.67	0	Rev
2,4-Dichlorophenol	3.65		7.89	4.34	3.06	4.32	3.93	1.69	Partly rev
2,4,6-Tribromophenol	1.84		6.8	4.97	4.13	4.70	4.927	1	Rev
Benzyltrimethylammonium Cl	5.28			0.7			0.775	0.522	Rev
Benzylamine	6		9.34	1.18	1.09	3.02	0.89	0.602	Rev/irrev
Aniline	4.56	1.13	4.6	2.01	0.9	2.99	1.45	–1.06	Rev
Benzamide	4.13	12.2		1.11	0.64	2.26	1.54	–0.301	Rev
2-Hydroxyethylether	6	2.31		–0.42	–1.47	0.15	–0.312	–1.08	Rev
2-Butanone	5.35	2.779		0.66	0.29	1.35	0.862	0	Rev
1,2-Diaminopropane	6		9.82	–0.1	–1.2	1.87	–0.318	–0.301	Irrev
2-Aminoethanol	6	2.27	9.50	0.25	–1.31	1.47		–1.36	Partly rev
Trichloroethylene	3.11			2.92	2.61	3.47	2.33	–0.602	Rev

(a)

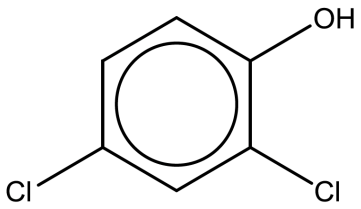

(b)

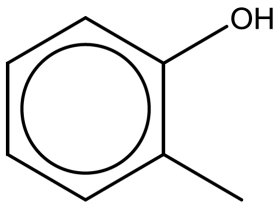

(c)

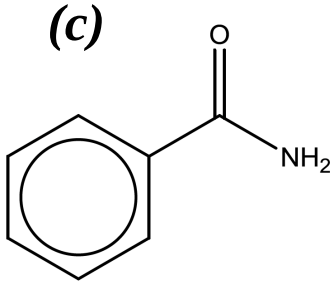

(d)

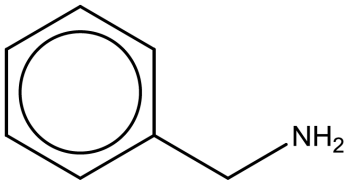

(e)

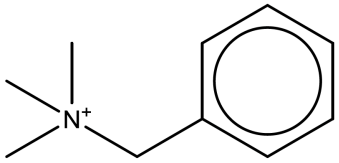

(f)

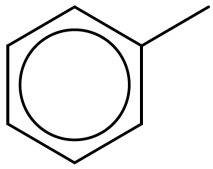

(g)

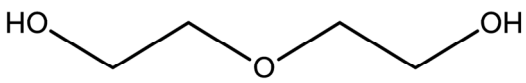

(h)

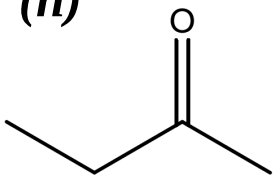

(i)

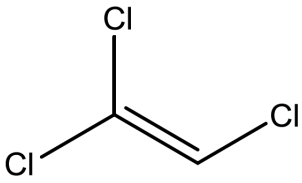

(j)

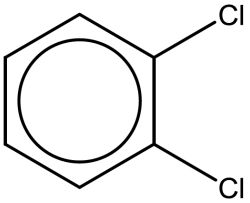

(k)

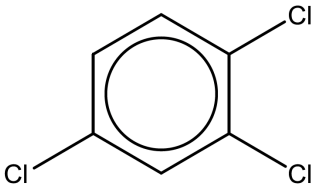

(l)

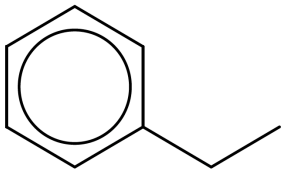

(m)

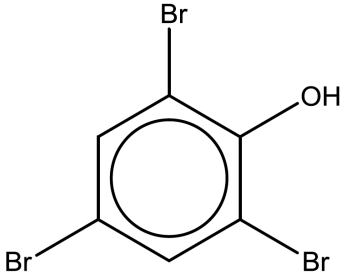

(n)

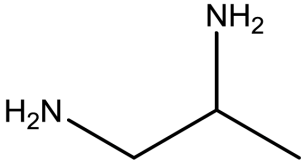

(o)

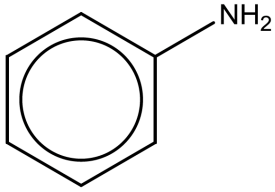

(p)

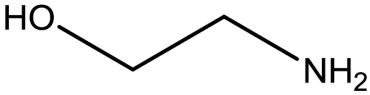

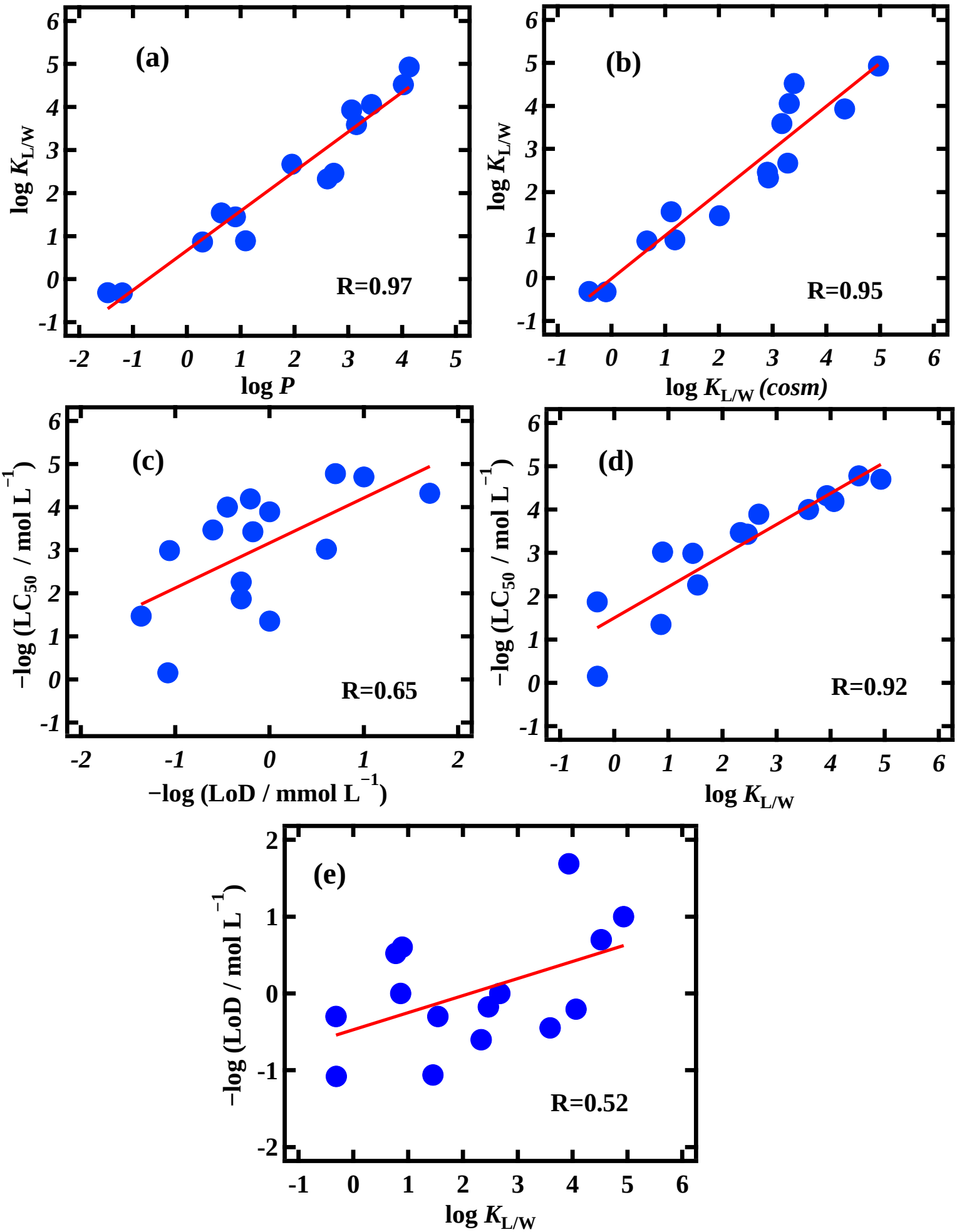
(a)
R=0.97
log $K_{L/W}$
log P
(b)
R=0.95
log $K_{L/W}$
log $K_{L/W}$ (cosm)
(c)
R=0.65
−log (LC$_{50}$ / mol L^{-1})
−log (LoD / mmol L^{-1})
(d)
R=0.92
−log (LC$_{50}$ / mol L^{-1})
log $K_{L/W}$
(e)
R=0.52
−log (LoD / mol L^{-1})
log $K_{L/W}$

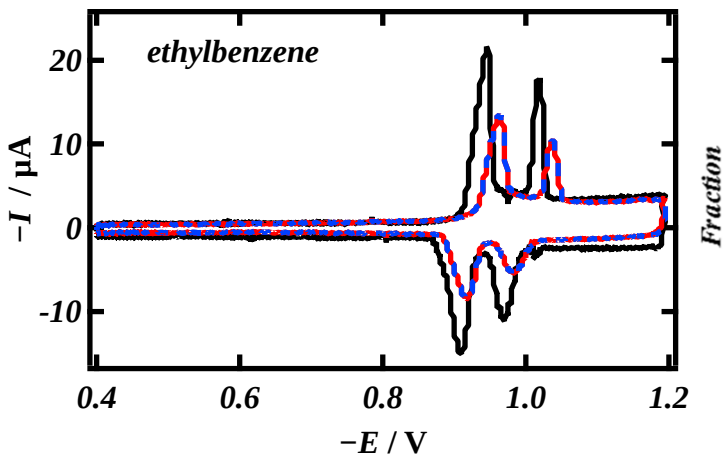
ethylbenzene
20
10
0
-10
−I / µA
0.4
0.6
0.8
1.0
1.2
−E / V

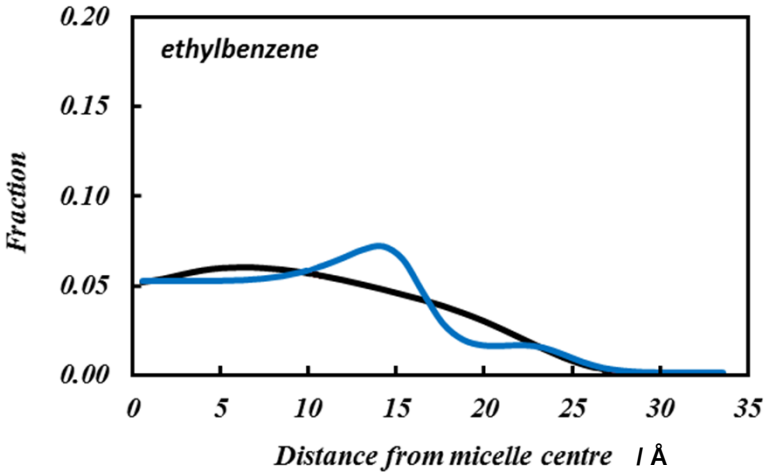
ethylbenzene
0.20
0.15
0.10
0.05
0.00
Fraction
0
5
10
15
20
25
30
35
Distance from micelle centre / Å

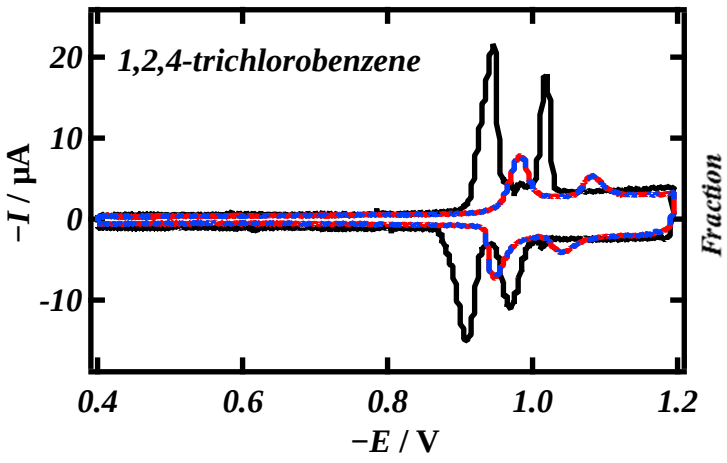
1,2,4-trichlorobenzene
20
10
0
-10
−I / µA
0.4
0.6
0.8
1.0
1.2
−E / V

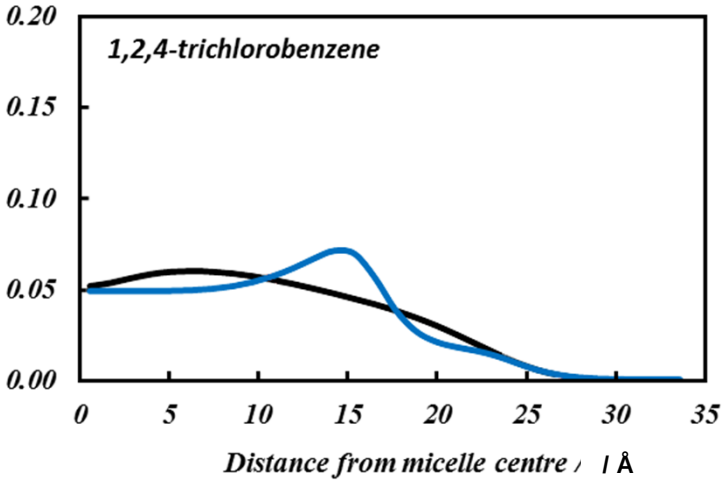
1,2,4-trichlorobenzene
0.20
0.15
0.10
0.05
0.00
Fraction
0
5
10
15
20
25
30
35
Distance from micelle centre / Å

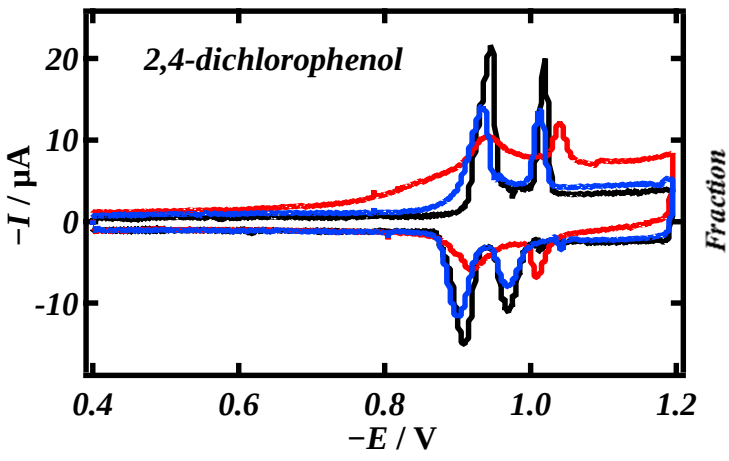
2,4-dichlorophenol
20
10
0
-10
−I / µA
0.4
0.6
0.8
1.0
1.2
−E / V

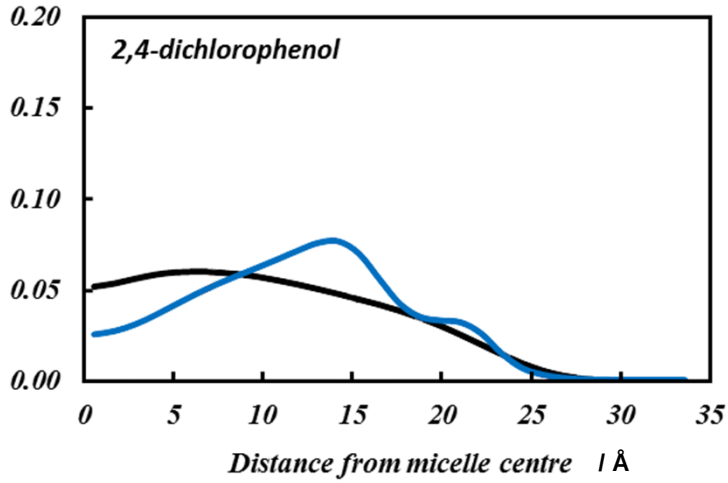
2,4-dichlorophenol
0.20
0.15
0.10
0.05
0.00
Fraction
0
5
10
15
20
25
30
35
Distance from micelle centre / Å

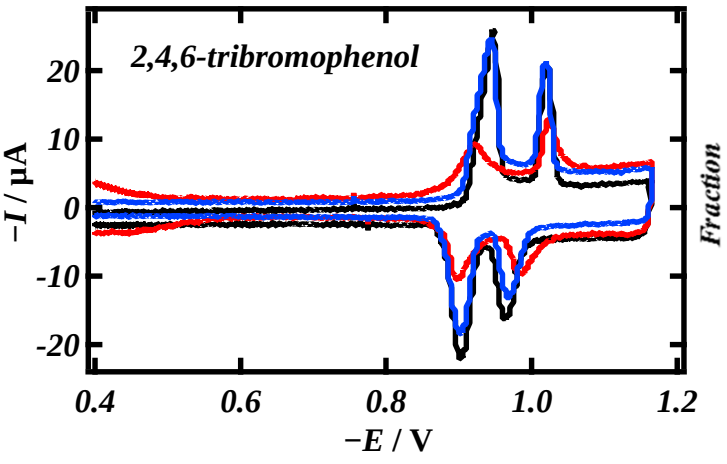
2,4,6-tribromophenol
20
10
0
-10
-20
−I / µA
0.4
0.6
0.8
1.0
1.2
−E / V

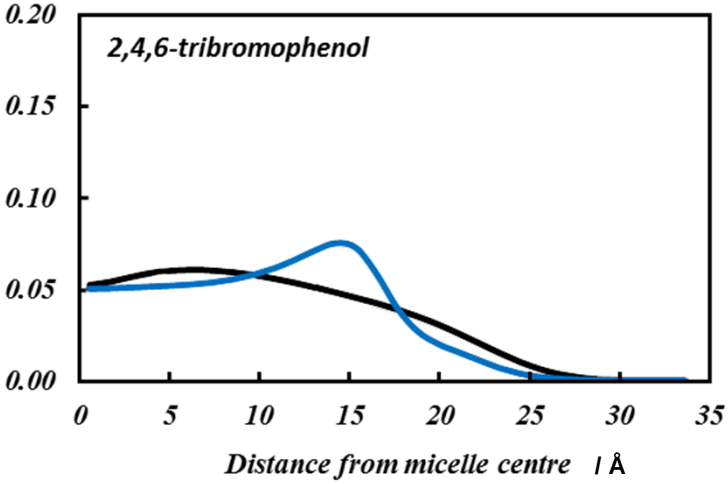
2,4,6-tribromophenol
0.20
0.15
0.10
0.05
0.00
Fraction
0
5
10
15
20
25
30
35
Distance from micelle centre / Å

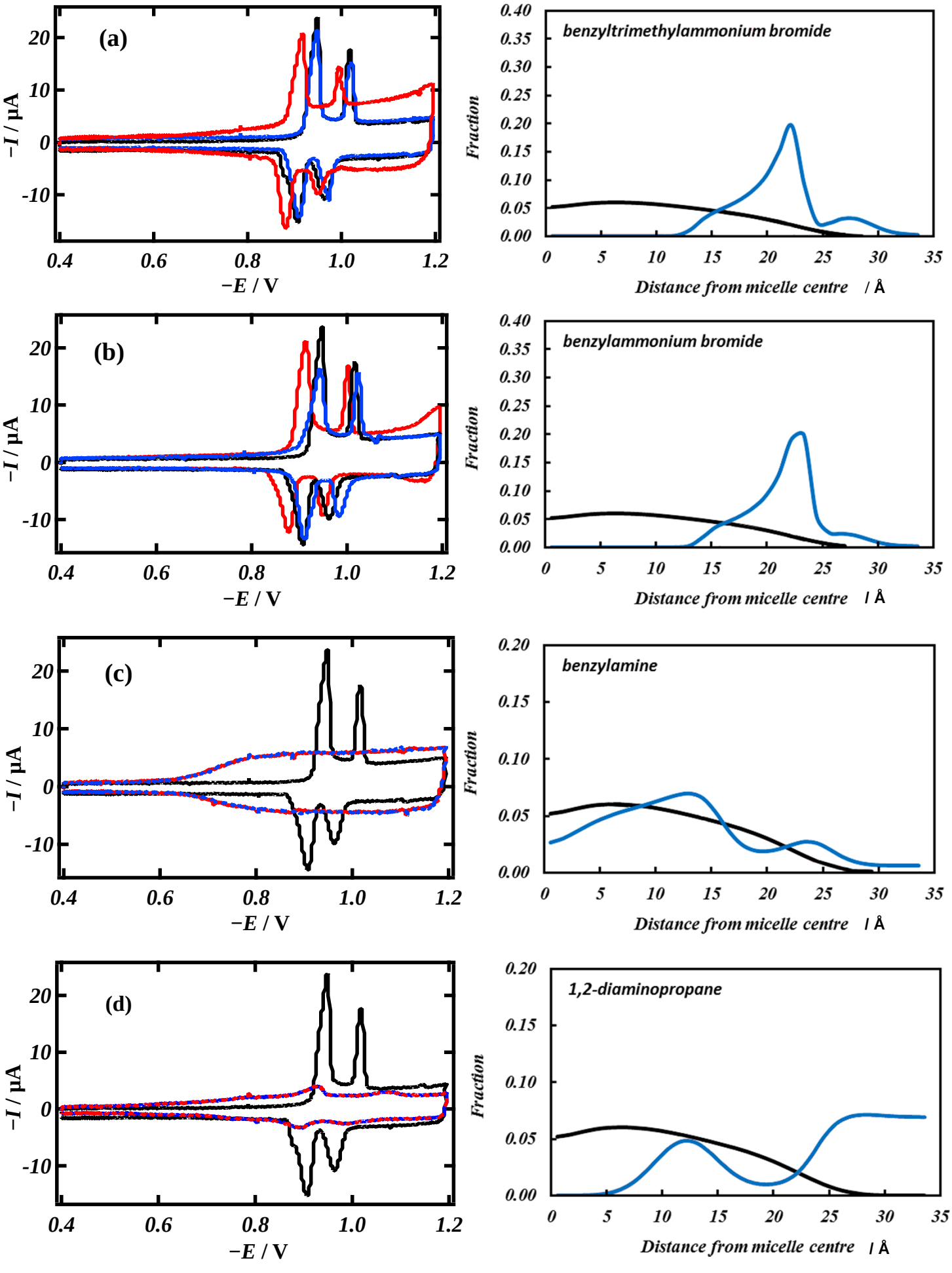
(a)
(b)
(c)
(d)
−I / μA
−E / V
Fraction
Distance from micelle centre / Å
benzyltrimethylammonium bromide
benzylammonium bromide
benzylamine
1,2-diaminopropane

Hg-supported phospholipid monolayer as rapid screening device for low molecular weight narcotic compounds in water

- DOPC on Hg sensor records molecular modification to phospholipid membranes
- Compound narcosis to fish is correlated with compound hydrophobicity
- Different structural classes of compound interact distinctively with lipid layer
- COSMOmic simulations validate the RCV signal for the compound/lipid interactions
- DOPC on Hg and IAM chromatography as integrated toxicity screening platform

Declaration of interests

☒ The authors declare that they have no known competing financial interests or personal relationships that could have appeared to influence the work reported in this paper.

☐The authors declare the following financial interests/personal relationships which may be considered as potential competing interests: